

# ANALYSIS OF CONTAMINANT DILUTION IN GROUNDWATER

Robert G. Baca, Gordon W. Wittmeyer, and Robert W. Rice

## 1 INTRODUCTION

Because of its importance to determining the degree of dose reduction, dilution of radionuclides in groundwater is likely to be a central issue in future performance assessments of the Yucca Mountain (YM) site. For example, if mixing of a contaminant stream with groundwater flow in the tuff aquifer dilutes the concentration by a factor of 100, then the dose (and associated radiologic risk) would be reduced by the same factor. Dilution of radionuclides released into the groundwater occurs as a result of fluid mixing along the flow path between the source point(s) and the location of the critical group(s). Mixing a dissolved contaminant (i.e., hydrodynamic dispersion) is, in general, strongly related to variations in both the magnitude of the fluid velocity and flow direction. These variations are principally caused by small and large scale heterogeneities in the geologic media (Gelhar, et al., 1985; Gelhar, 1993; Fetter, 1993). Large scale features, such as faults, may in some instances induce flow variations and thereby enhance natural mixing, while in other cases, they may produce highly channelized flow with limited mixing.

Defensible estimates of dilution factors for use in compliance demonstrations are expected to be derived by the U.S. Department of Energy (DOE) through an evaluation of available hydrochemical data, field tracer testing, and computer modeling (both abstracted and detailed). As used here, a dilution factor is the ratio of maximum steady-state radionuclide concentration at the source to the concentration at any point in the groundwater. With regard to detailed computer modeling, the nature and complexity of the geohydrologic system at the proposed site appears to merit a fully three-dimensional (3D) analysis of flow and transport. However, data requirements for a refined 3D analysis may pose a significant challenge to and redirection of certain site characterization activities at the YM site. Extensive characterization of the groundwater system could be especially important if highly accurate estimates of dilution become necessary to demonstrate compliance with a stringent groundwater protection requirement.

To date, only generic theoretical analyses of mixing and dilution have been performed by the DOE for the YM site (TRW Environmental Safety Systems Inc., 1995). These analyses suggest that natural or passive groundwater mixing will produce dilution factors on the order of  $10^3$  to  $10^5$  at 5 km (from the edge of the repository) and  $10^4$  to  $10^6$  at 30 km. These estimates are believed to be optimistic because (i) the technical bases were neither conservative or bounding, (ii) such large dilution factors imply a homogeneous hydrochemistry inconsistent with available data, and (iii) the dilution factors were much higher than those suggested by previous transport calculations in the DOE TSPA-93 (Wilson et al., 1994) that made use of much of the available hydrologic data. Estimates inferred from TSPA-93 calculations suggest dilution factors ranging from 5 to 20 at 5 km. These contrasting estimates of dilution are primarily because of distinct analysis approaches and differing assumptions for basic transport parameters (i.e., mass dispersivities, effective porosities). The DOE conducted tracer tests in the C-well complex (Geldon, 1995) that will yield important data that will be useful in refining dilution factor estimates.

In this scoping analysis, groundwater flow and transport models were used to study dilution characteristics of the proposed repository site for two basic purposes:

- gain insight into site specific factors that may affect groundwater mixing and attendant dilution of dissolved radionuclides at the YM site
- determine if there are any methodology issues that may impact implementation of a dose- or risk-based standard as proposed by the National Academy of Sciences (National Research Council, 1995)

The analysis presented herein was limited to consideration of only a few variations in the assumed hydraulic properties and boundary conditions. In addition, the geohydrologic system was treated as an equivalent porous continuum and no attempt was made to account for flow and transport through discrete fractures or to include matrix diffusion effects. Additionally, mixing induced by water well pumping was not considered. Because of the simplifications made and incompleteness of the site characterization, the calculations presented should not be viewed as an evaluation of regulatory compliance with existing standards.

## 2 ANALYSIS

To assess groundwater dilution and its dependence on the hydrogeologic characteristics of the YM setting, a series of two-dimensional (2D) computer simulations of groundwater flow and radionuclide transport was performed. Computer models were applied to compute four quantities: (i) hydraulic head distributions, (ii) flow paths, (iii) particle travel times, and (iv) radionuclide plume distributions. Dilution of technetium 99 ( $^{99}\text{Tc}$ ) was modeled because it is important to dose and reflects the dilution behavior of important radionuclides with relatively large inventories, long half-lives, and non-sorbing characteristics. Numerical calculations and graphical display of these four quantities were used to gain insight to the nature of the hydrogeologic processes that may control the degree of dilution at the YM site. Although available field data for the YM site are used, this scoping analysis did not consider uncertainties associated with the conceptualizations of groundwater flow or the spatial variability of hydraulic properties.

Two computer codes were used in performing the scoping analysis: MAGNUM-2D, a saturated flow model (England et al., 1985) and CHAINT, a multicomponent transport model (Kline and Baca, 1985). Hydraulic head distributions simulated with the MAGNUM-2D code were post processed to provide visualizations of the flow paths (i.e., streamlines) and particle travel times. Dilution factors calculated with the CHAINT code were contoured to depict plume spreading and dilution patterns. First, a 2D representation of planar flow from the repository site to the Amargosa Desert [i.e., the potential location of a farmer/rancher critical group (LaPlante et al., 1996)] was considered to assess the extent of hydrodynamic dispersion that may occur as the hypothetical  $^{99}\text{Tc}$  plumes move through relatively long and heterogeneous flow paths. A second 2D representation of a vertical cross section through the proposed repository site was also considered. The purpose of this case was to examine mixing processes immediately beneath the site that may occur as a result of channelized flow through the complex geometry of the hydrostratigraphic units and fault zones. Of particular interest was the extent to which structures such as fracture zones and faults control flow patterns, mixing, and dilution.

## 2.1 CONCEPTUAL MODELS OF GROUNDWATER FLOW

Conceptualizations of lateral and vertical flow used in this scoping analysis drew largely on information from previous DOE modeling studies (Czarnecki and Waddell, 1984; Wilson et al., 1994) and existing field data. The lateral flow model consisted of a 580 km<sup>2</sup> flow tube extending from the repository site south to Amargosa Desert. The vertical flow model approximates the cross section through the repository from borehole USW H-5 and extending through USW H-4; this cross section, which encompasses about 3 km<sup>2</sup>, is especially relevant because it appears to be aligned with the general direction of groundwater flow beneath the proposed repository site. Both the lateral and vertical flow conceptual models are defined in terms of

- geometry of the hydrostratigraphic units
- contrasting values of saturated hydraulic conductivity
- variability of effective porosity
- location of distinct fault zones
- hydraulic head gradient and flow boundary conditions.

The specific aspects of the two conceptual models are summarized in the following sections.

### 2.1.1 Conceptual Model of Lateral Flow in the Yucca Mountain Region

In developing a 2D lateral flow model, computer simulation results previously published by the U.S. Geological Survey (USGS) (Czarnecki and Waddell, 1984) were examined and used. Czarnecki and Waddell (1984) applied a vertically integrated, steady-state model to simulate the regional flow system. These authors present a plot of the groundwater flux vectors that were computed from the hydraulic head field (see plate 2 in Czarnecki and Waddell, 1984). A subdomain of the Czarnecki and Waddell (1984) regional flow model was selected by tracing selected streamlines west and east of the proposed repository. Locations of the upper and lower boundaries of this streamtube were taken coincident with head contours of 800 m and 675 m, respectively, as estimated from available field measurements. The streamtube, which is shown in figure 2-1, was divided into seven distinct material types or zones; each of these zones is designated by a number (see circled numbers). Boundaries for the seven zones (designated by dashed lines) were determined by inspecting available hydrostratigraphic cross sections (Gillson et al., 1995; Roberson et al., 1995) and hydraulic head contours.

Estimates of the horizontal hydraulic conductivities  $K_{xx}$  and  $K_{yy}$  were obtained by a manual calibration procedure in which the hydraulic conductivities of the seven zones were adjusted until the MAGNUM-2D code produced a reasonable fit with measured hydraulic heads (Robison, 1984; and Ervin et al., 1993). These initial estimates were subsequently checked and adjusted using an autocalibration algorithm that employed an indirect inverse procedure based on either maximum likelihood or statistically robust M-estimator theory to estimate model parameters (Wittmeyer, 1990; Wittmeyer and Neuman, 1992; and Carrera and Neuman, 1986a,b,c). Within the selected flow domain (see figure 2-1) there were 146 locations at which estimates of hydraulic head data were available. Of these measurements, 22 were in the general vicinity of YM, 5 just west of the town of Lathrop Wells, and the remaining 119 in the

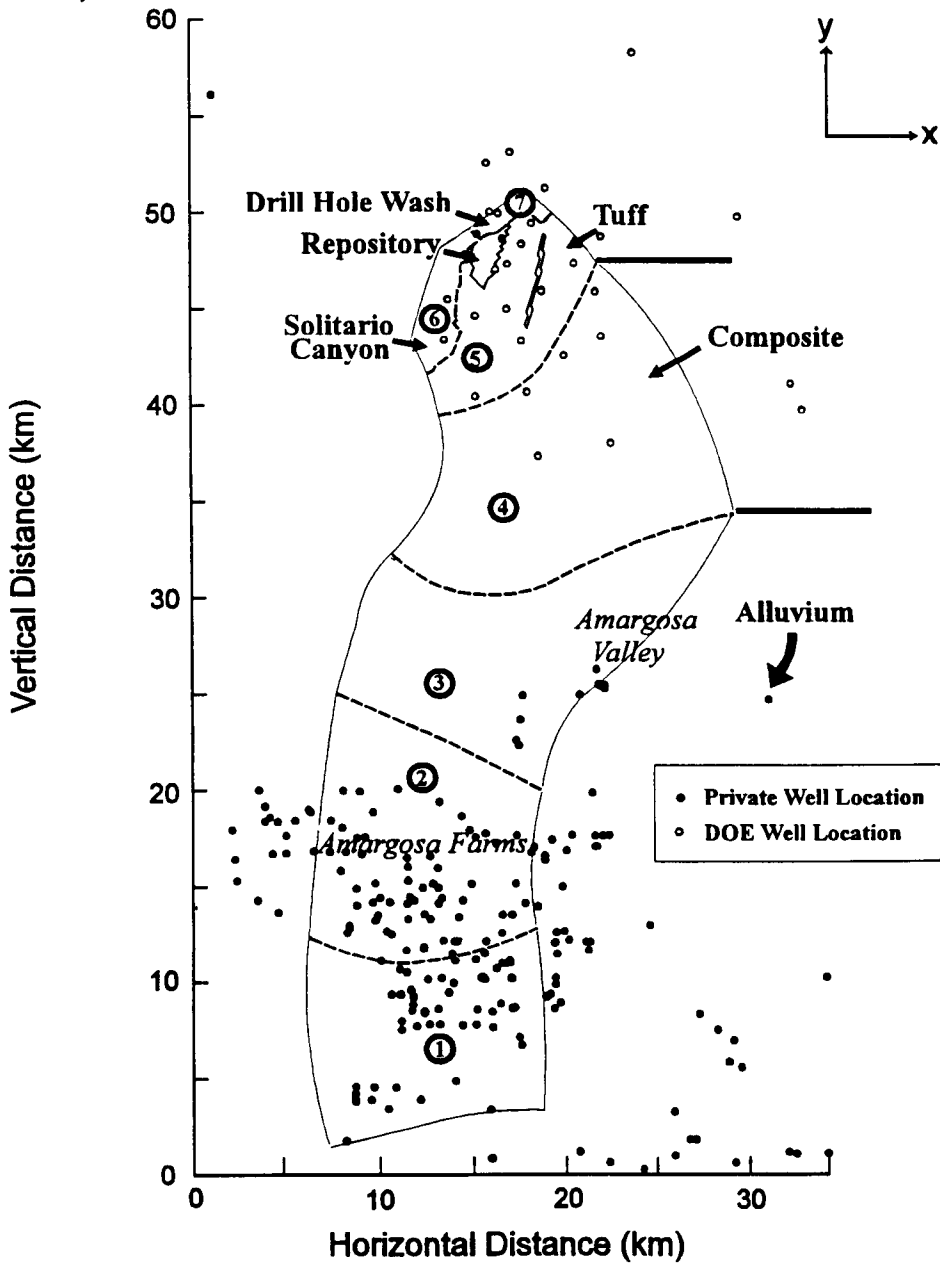


Figure 2-1. Location of lateral flow model, material zones (circled numbers), well locations, and location of the repository foot print

Amargosa Farms region. Within each of the seven zones, the hydraulic conductivity was assumed uniform and isotropic.

Because the lateral flow model used two Dirichlet and two no-flow boundary conditions, the values of hydraulic conductivity in the seven major zones are not uniquely identifiable in the absence of prior estimates of either areal flux or hydraulic conductivity (Carrera and Neuman, 1986b). Inasmuch as areal recharge within this region is minimal, fixing at least one hydraulic conductivity value was judged the best option. Accordingly, Zone 1, located at the southern end of the streamtube model, was assigned a fixed hydraulic conductivity value of  $1.7 \times 10^{-5}$  m/s, consistent with the estimate of Czarnecki (1985). In order to assess the fit between predicted and observed values, the hydraulic head residual was calculated for each well location. The head residuals ranged from -38.4 to 62.3 m, with an average head residual of 1.4 m and an average absolute head residual of 6.3 m (the head residual is equal to the head value predicted by the streamtube model minus the measured head value). An improved fit could have been achieved by increasing the number of zones; however, the selected zonation was considered adequate for this 2-D scoping analysis. The seven zones and assumed hydraulic properties are summarized in table 2-1.

After completing the calibration of the flow model, an additional zone representing the Bow Ridge fault was added to the conceptual model, with hydraulic properties assigned to represent two contrasting cases:

- (i) preferential flow along the fault and partial barrier to flow across the fault (i.e.,  $K_{xx}$  and  $K_{yy}$  set to  $10^{-7}$  and  $10^{-5}$  m/s, respectively),
- (ii) barrier to groundwater flow (i.e.,  $K_{xx}$  and  $K_{yy}$  set to  $10^{-8}$  m/s).

These two cases produced distinct flow paths, particle travel times, and plume dilution patterns in the vicinity of the proposed repository.

In addition to the hydraulic conductivities discussed previously, calculation of groundwater velocity and plume dilution required estimates of "effective porosity" (i.e., the portion of the total porosity participating in the transmission of water). At present, there are no field data for effective porosities of the tuff formations or the alluvium at the YM site. Fracture porosity, estimated using the cubic law (Snow, 1969) and observed fracture porosities, is one surrogate for effective porosity. Erickson and Waddell (1985) estimated fracture porosities of productive zones in the tuff aquifer to range from about  $10^{-4}$  to  $10^{-3}$ ; this range was estimated using transmissivity data for fracture zones from borehole USW H-4. In an unconfined system, the specific yield is another surrogate parameter for effective porosity (Domenico and Schwartz, 1990). The USGS obtained specific yield data for the tuff aquifer (Geldon, 1995) in boreholes east of the proposed repository site and for the alluvium (Walker and Eakin, 1963) in the vicinity of the Amargosa Valley. In the calculations presented, the specific yield data were used to provide representative estimates of effective porosity,  $\phi$ .

The C-well complex (Geldon, 1995) of boreholes (i.e., UE-25c #1, UE-25c #2, and UE-25c #3), located on the east flank of the YM site, penetrate the saturated Calico Hills aquifer, Upper Prow Pass confining unit, the Prow Pass-Upper Bullfrog aquifer, the Middle Bullfrog confining unit, the Bullfrog aquifer, the Lower Bullfrog confining unit, and the Tram aquifer. Geldon (1995) analyzed two well interference tests conducted in the Calico Hills and Prow Pass-Upper Bullfrog aquifers using the

Table 2-1. Estimates of hydraulic conductivities computed using autocalibration technique

Zone	Hydraulic Conductivity (m/s)	
	$K_{xx}$	$K_{yy}$
1—Alluvium	$1.7 \times 10^{-5}$	$1.7 \times 10^{-5}$
2—Alluvium	$8.6 \times 10^{-6}$	$8.6 \times 10^{-6}$
3—Alluvium	$4.5 \times 10^{-6}$	$4.5 \times 10^{-6}$
4—Composite (Alluvium/Tuff)	$1.7 \times 10^{-5}$	$1.7 \times 10^{-5}$
5—Tuff Aquifer	$1.1 \times 10^{-5}$	$1.1 \times 10^{-5}$
6—Solitario Canyon	$7.4 \times 10^{-7}$	$7.4 \times 10^{-7}$
7—Drill Hole Wash	$2.0 \times 10^{-9}$	$2.0 \times 10^{-9}$

Neuman (1975) type curve method for an unconfined, anisotropic aquifer. Type curve analysis of heads measured in UE-25c #1 with pumping in UE-25C #2 indicated that the specific yield for the unconfined Calico Hills aquifer is 0.003 (Geldon, 1995). The Prow Pass-Upper Bullfrog aquifer may either be confined or unconfined in UE-25C #1. If unconfined, the Prow Pass-Upper Bullfrog aquifer has a specific yield of 0.004 (Geldon, 1995). For a field test where UE-25c #3 was pumped with heads monitored in UE-25c #2, the specific yield for the composite column was estimated to be 0.07 (Geldon, 1995). Thus, for those portions of the planar flow model in which the upper 100 to 300 m of the saturated zone is contained in the fractured volcanics, effective porosity was assumed to be bounded by  $0.003 \leq \phi \leq 0.07$ .

For the remaining zones of the model domain, effective porosities for the alluvium were inferred from specific yield estimates made by Walker and Eakin (1963) for the Amargosa Desert. These authors estimated the average specific yield to be 0.17 from textural descriptions from driller's logs for 57 wells in the Amargosa Desert. Walker and Eakin (1963) also noted that the variation in physical conditions throughout the Amargosa Desert would suggest that the specific yield ranges from about 0.10 to 0.20. Accordingly, the effective porosity for these portions of the flow domain model was assumed to be bounded by  $0.10 \leq \phi \leq 0.20$ . It is important to acknowledge that the effective porosities of alluvium can be much larger than 0.20 [e.g., 0.30 to 0.40 (Freeze and Cherry, 1979; Domenico and Schwartz, 1990)]. The significance of this observation is that larger values of effective porosities result in larger particle travel times.

### 2.1.2 Conceptual Model for Vertical Flow Beneath the Yucca Mountain Site

To develop a 2D representation of flow in the tuff aquifer beneath the proposed repository site, the geologic cross section (see figure 2-2) developed by the USGS (Scott and Bonk, 1984) was used. This

cross section clearly illustrates the heterogeneous nature and complex geometry of the strata beneath the YM site, which is expected to influence mixing and dilution. The cross section depicts the slightly east dipping hydrostratigraphic units of the tuff aquifer as well as the Ghost Dance and Bow Ridge fault zones. To simplify the generation of the computational grid, various secondary faults in this cross section were not explicitly modeled. This northwest to southeast cross section, which passes through boreholes USW H-5 and USW H-4, is particularly relevant because it is oriented along the principal direction of groundwater flow and through the center of the proposed repository site.

The location of the upper boundary of the conceptual model was obtained by interpolation of available borehole data. Both the upper and lower boundaries of the model domain were treated as no-flow boundaries. The hydraulic heads at the inflow and outflow boundaries were set to impose an average hydraulic gradient of  $3.4 \times 10^{-3}$ . This gradient was estimated from the steady-state hydraulic head field calculated for the planar flow model. The hydraulic conductivities assigned to the individual hydrostratigraphic units were largely drawn from the field data for borehole USW H-4 presented in Whitfield et al. (1985). A hydraulic conductivity profile for USW H-5 was not available because the field test results were apparently too difficult to interpret (Robison and Craig, 1991) possibly because of the hydraulic influence of high-angle fractures near the borehole. The effective porosities assigned to the units were consistent with those used in the planar flow model.

The hydraulic conductivity profile measured in borehole USW H-4 (Whitfield et al., 1985) was used to assign properties to individual hydrostratigraphic units. Whitfield et al. (1985) report pump test data for 19 individual hydrostratigraphic units. For simplicity, certain adjacent flow zones with similar hydraulic conductivities were lumped together. This produced a simpler hydrostratigraphic model consisting of 11 major zones. To account for anisotropic characteristics of these strata, an anisotropy ratio (i.e., ratio of vertical hydraulic conductivity  $K_z$  to the horizontal hydraulic conductivity  $K_x$ ) of 1 to 5 was assumed. This assumption had the effect of emphasizing channelized flow along the hydrostratigraphic units. The Bow Ridge fault was represented as an anisotropic feature in the conceptual model. The hydraulic conductivity values assumed for the hydrostratigraphic model are summarized in table 2-2.

## 2.2 COMPUTER SIMULATIONS FOR LATERAL FLOW MODEL

Steady-state representations of the potentiometric field for the lateral flow model were generated for two cases in which the Bow Ridge fault was treated as a preferential flow pathway and a flow barrier. The hydraulic head fields calculated (with the MAGNUM-2D code) for both cases were post-processed to obtain head contours, flow vectors, Darcy fluxes, streamlines, and cumulative particle travel times. Flow paths, for particles released at locations along a line tangential to the lower boundary of the repository foot print, were plotted to provide a visualization of groundwater flow patterns. Along each flow path (or streamline), the particle travel time was calculated and summed to give an indication of the impact of velocity variations.

The formation and movement of hypothetical  $^{99}\text{Tc}$  plumes were computed (with the CHAINT computer code) for  $10^4$  yr using a longitudinal mass dispersivity ( $\alpha_L$ ) of 200 m and transverse mass dispersivity ( $\alpha_T$ ) of 10 m. The longitudinal dispersivity value was selected by examining dispersivity data plotted in Gelhar (1993) which displays the relation between  $\alpha_L$  and the scale of observation; the selected value is about 1/5 of that used by DOE (Wilson et al., 1994) in radionuclide transport simulations for

## Geologic Cross-section

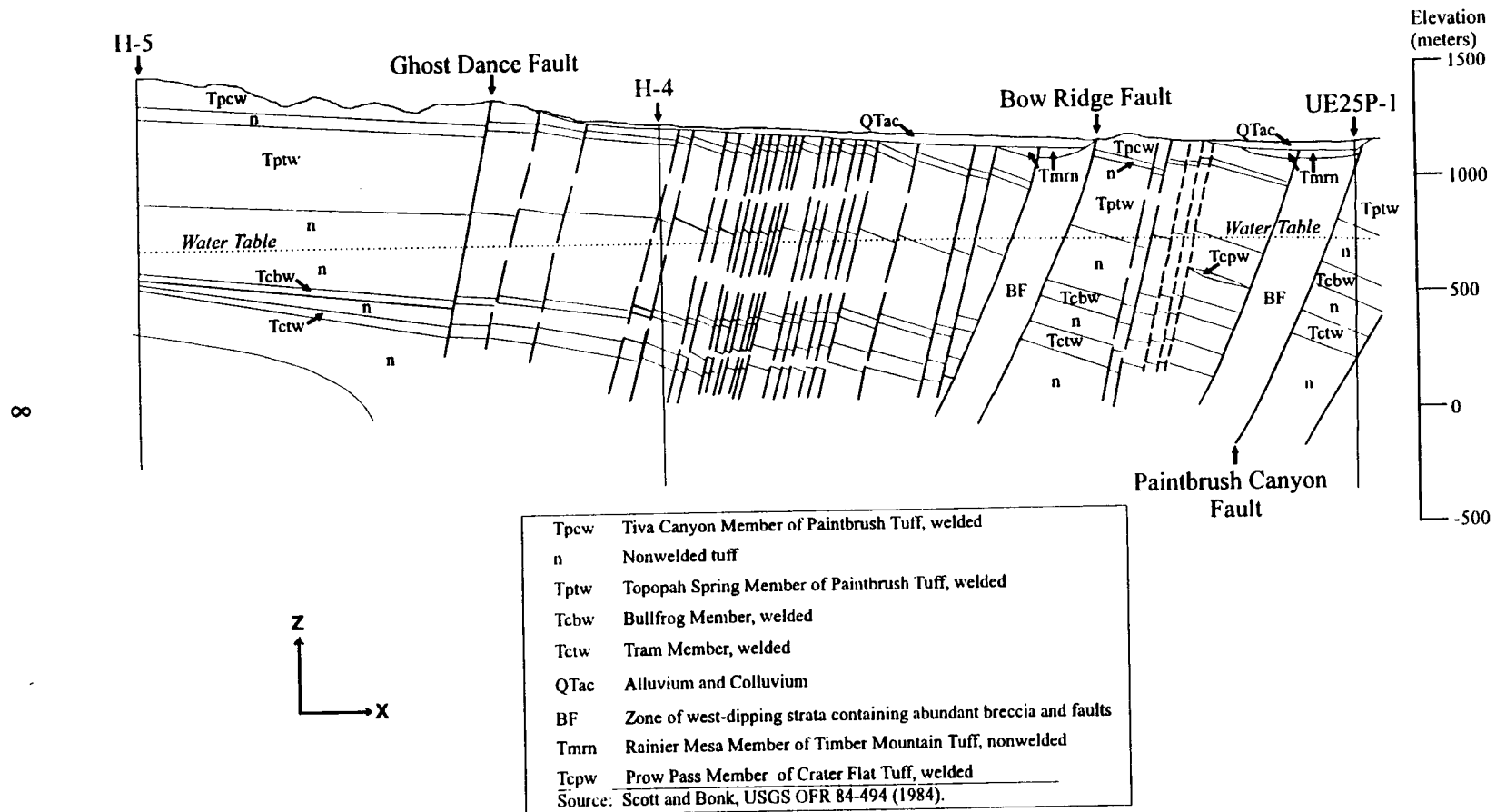


Figure 2-2. Vertical cross section through boreholes USW H-5 and USW H-4 (Scott and Bonk, 1984)

6/29

10/29

**Table 2-2. Assumed hydraulic conductivities for the vertical cross section model, based on data presented by Whitfield et al. (1985)**

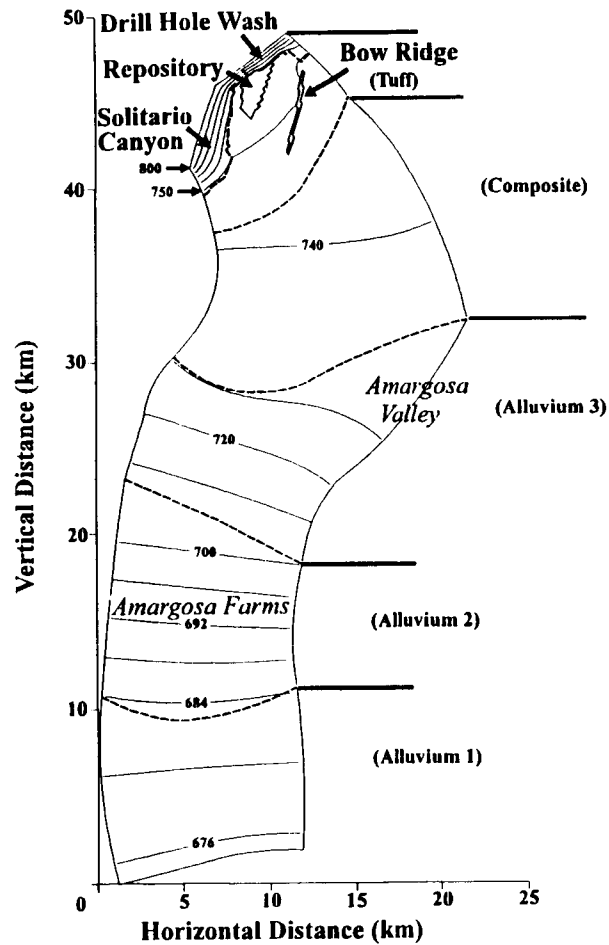
Zone	Hydraulic Conductivity (m/s)	
	$K_{xx}$	$K_{zz}$
1—Calico Hills (CH)	$1.0 \times 10^{-6}$	$2.0 \times 10^{-7}$
2—Prow Pass #1 (PP1)	$1.0 \times 10^{-5}$	$2.0 \times 10^{-6}$
3—Prow Pass #2 (PP2)	$2.0 \times 10^{-6}$	$4.0 \times 10^{-7}$
4—Bull Frog #1 (BF1)	$2.0 \times 10^{-5}$	$4.0 \times 10^{-6}$
5—Bull Frog/Tram (BF/TR)	$4.0 \times 10^{-6}$	$8.0 \times 10^{-7}$
6—Tram #1 (TR1)	$2.0 \times 10^{-5}$	$4.0 \times 10^{-6}$
7—Tram #2 (TR2)	$2.0 \times 10^{-6}$	$4.0 \times 10^{-7}$
8—Tram #3 (TR3)	$2.0 \times 10^{-5}$	$4.0 \times 10^{-6}$
9—Tram #4 (TR4)	$1.0 \times 10^{-6}$	$2.0 \times 10^{-7}$
10—Lithic Ridge #1 (LR1)	$2.0 \times 10^{-5}$	$4.0 \times 10^{-6}$
11—Lithic Ridge #2 (LR2)	$2.0 \times 10^{-6}$	$4.0 \times 10^{-7}$
12—Bow Ridge Fault	$1.0 \times 10^{-7}$	$5.0 \times 10^{-7}$

the proposed repository site. The transverse dispersivity was computed as  $\alpha_T = \alpha_L / 20$  following Fetter (1993).

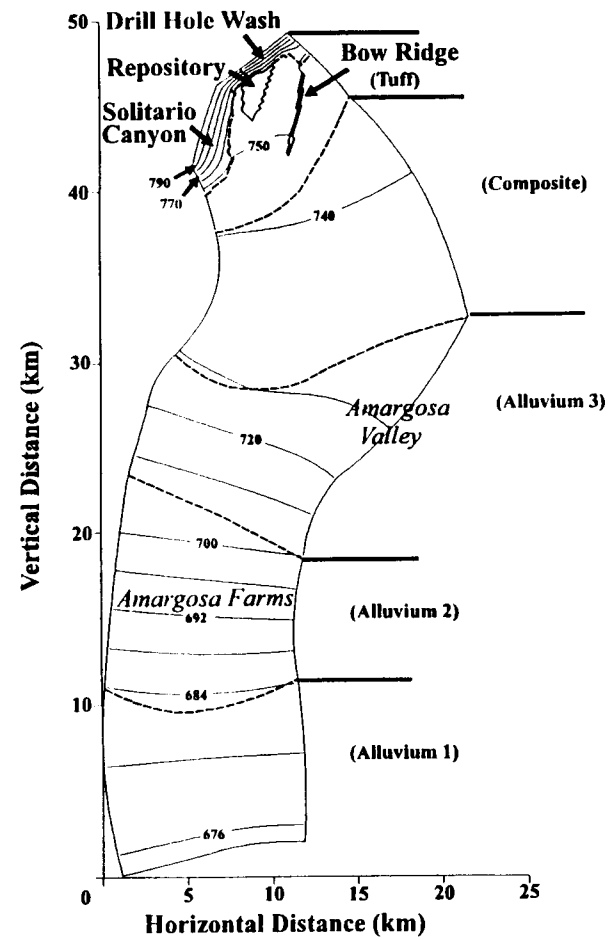
A relatively fine grid, consisting of more than 6,000 elements, was used to represent the flow domain. This fine grid was used to minimize numerical dispersion. The following sections present and interpret the significance of subregional flow path and particle travel times and plumes and dilution factors. A range of computer simulations was made for this conceptualization; however, only selected cases are presented.

### 2.2.1 Hydraulic Heads, Flow Vectors, and Darcy Fluxes

Patterns of subregional groundwater flow are determined by the combined effects of the hydraulic boundary conditions, geometry of flow domain, contrasts in hydraulic properties, and structural features such as fault zones. Some of these effects are illustrated in the contour plot of the hydraulic head field shown in figure 2-3; the dashed and heavy solid lines designate the material zone boundaries within the flow domain. In both cases, the hydraulic heads exhibit large gradients to the west (Solitario Canyon)



(a) preferential flow pathway



(b) flow barrier

Figure 2-3. Hydraulic head fields for the lateral flow model for two cases with the Bow Ridge fault assumed to be (a) preferential flow pathway and (b) flow barrier

6/2/11

12/29

and north (Drill Hole Wash) of the repository and then transition to more gradual variations in the tuff (zone 5), composite (zone 4), and alluvial regions (zones 1, 2, and 3). In comparing the head fields for the two cases, the hydraulic characteristics assigned to the Bow Ridge fault only appear to have local and relatively small effects.

Flow vector plots for the two cases are shown in figure 2-4 along with the tabulated ranges for the Darcy fluxes; note that the flux magnitude is indicated by the arrow length. The principal differences in calculated results are confined to a small region between the proposed repository and Bow Ridge fault. For the preferential flow pathway case, groundwater flow occurs along and through the fault. In contrast, the flow barrier case shows that flow is routed around the fault. Particularly noteworthy was the fact that between the two cases the range of flux magnitudes were not substantially different, except in the Bow Ridge fault zone where differences were expected. Also presented in the figure are the Darcy fluxes (maximum and minimum values) computed for each zone. In the proposed repository zone, the calculated fluxes for both cases range from about 0.5 m/yr to 1.9 m/yr. The largest flux magnitude is 3.7 m/yr in the tuff aquifer (i.e., zone 5).

### 2.2.2 Pathlines, Particle Travel Times, and Dilution Factors

Flow paths calculated for particles released along the border of the repository provide insight into the subregional flow patterns. As can be seen in figure 2-5, the streamlines for the preferential flow pathway case refract as they pass through Bow Ridge fault; whereas, for the flow barrier case, the streamlines flow around the fault. The isopleths (heavy dashed lines) of constant particle travel time (also shown in this figure) add additional detail to the contrasting effects of the fault. These isopleths depict the relative rate of travel of particles moving passively with the groundwater. It is clear from these isopleths that patterns of groundwater flow in the vicinity of the fault are quite distinct for the two cases considered. However, these distinct flow patterns appear to have relatively small local effects on lateral mixing and almost no observable influence on the larger scale transport; this is more clearly shown in the subsequent figure.

The impact of local and subregional flow patterns on contaminant movement is illustrated in the contour plot of  $^{99}\text{Tc}$  (see figure 2-6); the isopleths are quantified in terms of dilution factors instead of radionuclide concentrations. Plume representations for a snapshot in time at  $10^4$  yr after release are shown in the figure. The contour plots suggest local mixing and dilution in the vicinity of the repository is relatively small (i.e., dilution factors are about 2). Significant in both cases is that predicted dilution factors in the Amargosa Farms region are about the same.

## 2.3 COMPUTER SIMULATIONS FOR VERTICAL FLOW MODEL

A steady-state hydraulic head field was generated with the MAGNUM-2D code using the boundary conditions and hydraulic properties described previously. The calculated hydraulic head field was contoured as well as post-processed to obtain flow vectors, Darcy fluxes, streamlines, and cumulative particle travel times. Flow paths for particles released at selected locations along the Ghost Dance fault were computed to provide a visualization. Along each flow path, the particle travel time was calculated and summed to give an indication of the influence of velocity variations.

The formation and movement of the hypothetical  $^{99}\text{Tc}$  plumes were computed with the CHAINT computer code using a longitudinal dispersivity ( $\alpha_L$ ) of 30 m and transverse dispersivity ( $\alpha_T$ ) of 3 m.

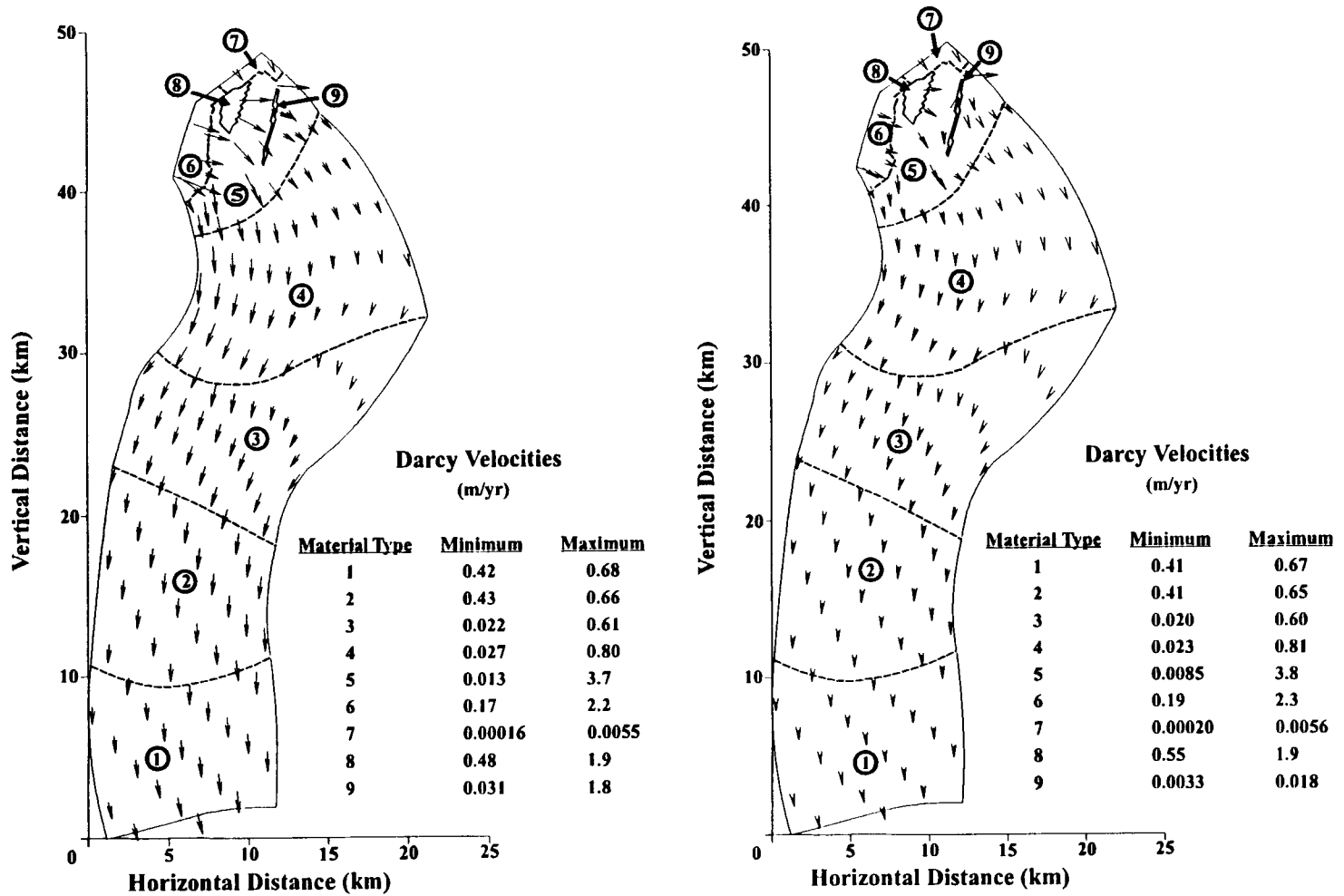
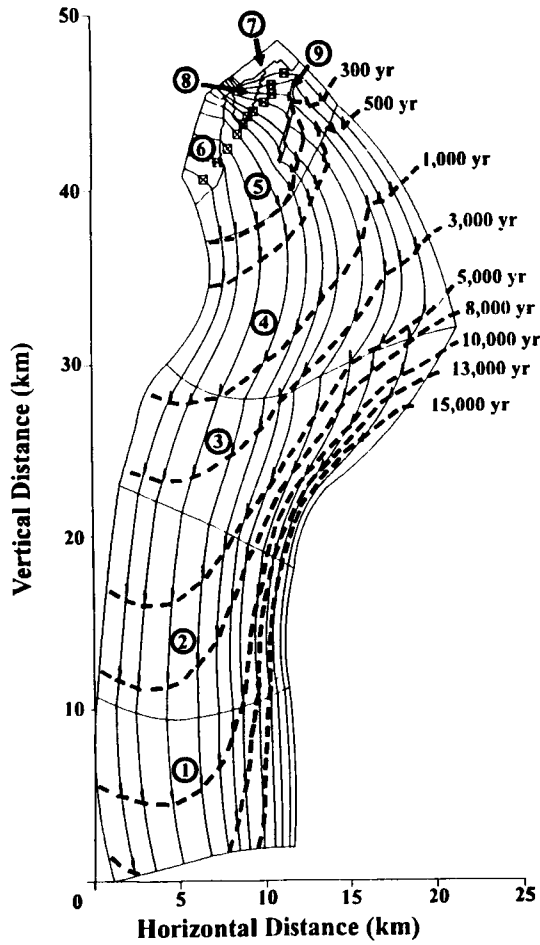
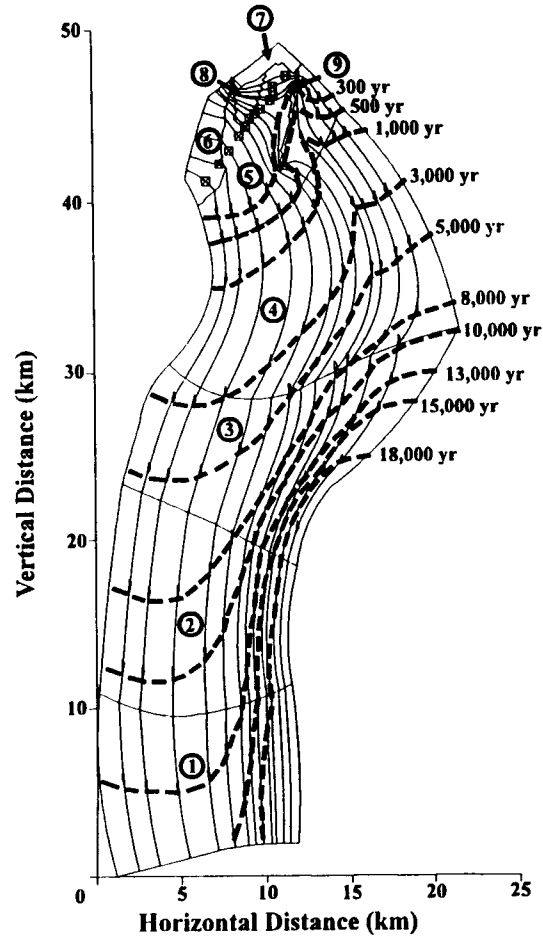


Figure 2-4. Darcy flux vector plots for lateral flow model for two cases with the Bow Ridge fault assumed to be (a) preferential flow pathway and (b) flow barrier

13/29



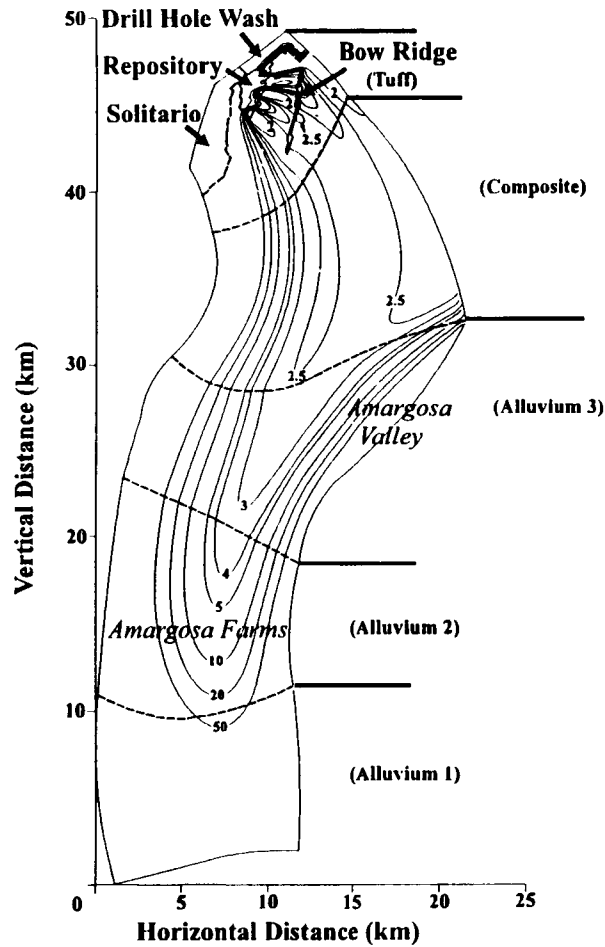
(a) preferential flow pathway



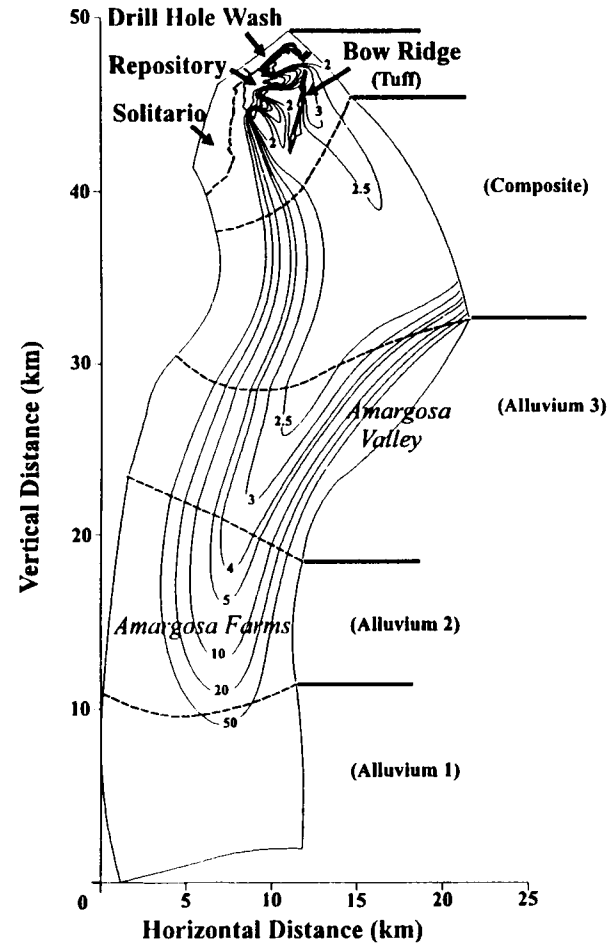
(b) flow barrier

Figure 2-5. Pathlines and particle travel times for lateral flow model for two cases with the Bow Ridge fault assumed to be (a) preferential flow pathway and (b) flow barrier

14/9/9



(a) preferential pathway



(b) flow barrier

Figure 2-6. Radionuclide plume distributions for lateral flow model for two cases with Bow Ridge fault assumed to be (a) preferential flow pathway and (b) flow barrier; contour levels are in terms of dilution factors

The mass dispersivities were chosen to be smaller than those used in the lateral flow model because of the shorter length of the flow domain (i.e., smaller scale of observation). The longitudinal dispersivity was chosen to be consistent with the value used in Nuclear Regulatory Commission (1995) while the transverse dispersivity was taken as  $\alpha_T = \alpha_L/10$ ; a slightly larger transverse to longitudinal dispersivity ratio was assumed to reduce gridding requirements.

A relatively fine grid, consisting of more than 8,000 elements, was used to represent the flow domain. This fine grid was used to minimize numerical dispersion. The following sections present and interpret the significance of (i) local flow path and particle travel times and (ii) plumes and dilution factors. A range of computer simulations was made for this conceptualization; however, only selected cases are presented.

### 2.3.1 Hydraulic Heads, Flow Vectors, and Darcy Fluxes

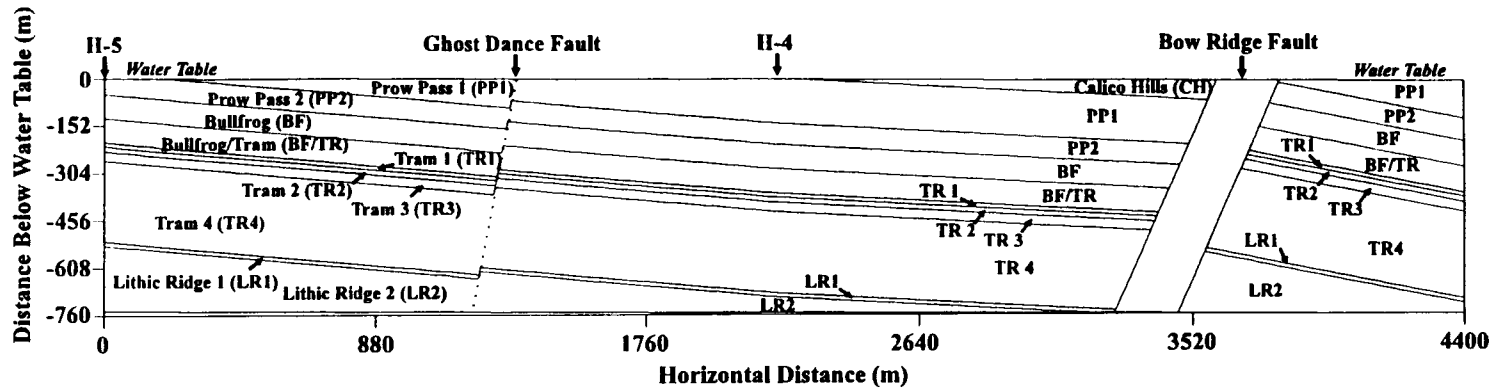
Patterns of vertical groundwater flow in the tuff aquifer are determined by the combined effects of the hydraulic boundary conditions, geometry of the strata (e.g., dipping layers), and the presence of discontinuities associated with fault zones. These effects are illustrated in the contour plot of the hydraulic head field shown in figure 2-7; the nomenclature used in the figure is consistent with Whitfield et al. (1985). Although the boundary conditions are in fact uniform, the contours indicate the head field becomes reoriented. In some locations, the plot suggests that the hydraulic head fields adjusted to move water along the most conductive hydrostratigraphic units. In contrast, the hydraulic head field in the lower permeability units is oriented in such a manner as to gradually move water up, toward more conductive units. Very high local gradients develop in the vicinity of the Bow Ridge fault, indicating that this feature acts as a partial flow barrier.

Additional insights into the vertical flow field were obtained by computing and plotting the velocity vectors (see figure 2-8). The presence of the Ghost Dance fault appears to have little or no effect on the flow field, whereas the Bow Ridge fault zone produces a distinct downward flow field. Downstream of the Bow Ridge fault, the flow field becomes upward trending, negating the effects of the downward dipping hydrostratigraphic units. Also presented in figure 2-8 are the calculated ranges of Darcy fluxes computed for each unit. In the vicinity of the water table, the maximum fluxes are estimated to be about 1.3 m/yr in the Prow Pass unit and about 1.5 m/yr in the Bullfrog unit. The largest flux (i.e., 2.9 m/yr) occurs in the Lithic Ridge unit located about 500 m below the water table.

### 2.3.2 Flow Paths, Particle Travel Times, and Dilution Factors

The flow paths calculated for particles released along the Ghost Dance fault confirm interpretations drawn from flow vectors. As can be seen in figure 2-9, the streamlines near the water table in the Prow Pass unit are horizontal and then dip down avoiding flow within the lower permeability Calico Hills unit. These streamlines dip down, as they cross the Bow Ridge fault zone but return to levels very near the water-table surface. Also shown in figure 2-9 are isopleths (heavy dashed lines) of constant particle travel time. These depict the relative rate of particle travel through the groundwater system. It is clear from these isopleths that groundwater movement is highly nonuniform in both the Prow Pass and Bullfrog units. This pattern of flow suggests that contaminants entering the aquifer would be transported primarily along the surface of the water table with vertical mixing only occurring in areas where there are large changes in flow direction (i.e., Bow Ridge fault).

### Hydrostratigraphic Model



16

### Hydraulic Head Contours (m)

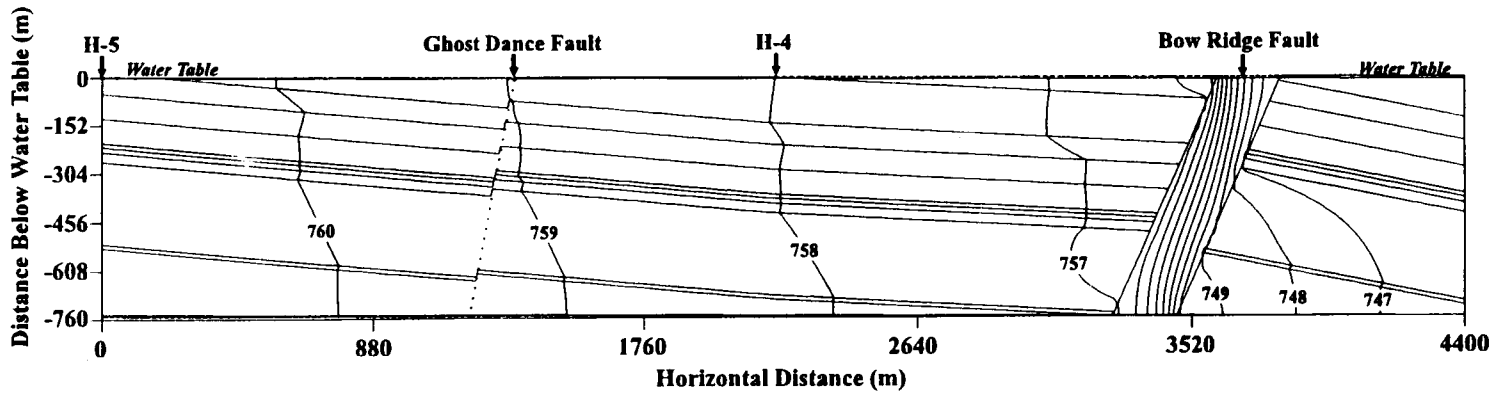
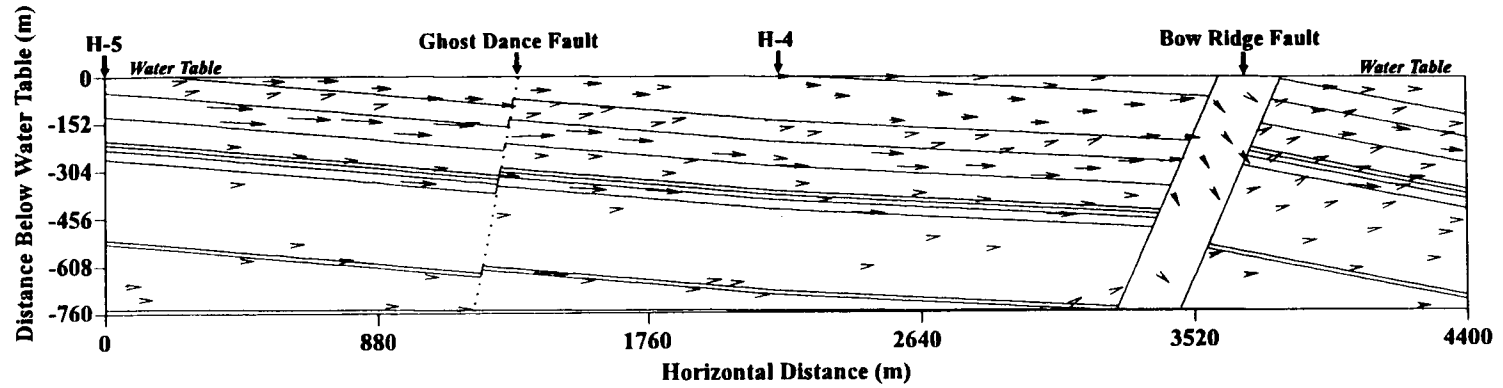


Figure 2-7. Hydraulic head fields for vertical cross section model; stratigraphic nomenclature taken from Whitfield et al. (1985)

17/99

### Darcy Velocity Vectors



### Darcy Velocities (m/yr)

Material Type	Minimum	Maximum
Calico Hills (CH)	0.030	0.79
Prow Pass 1 (PP1)	0.015	1.3
Prow Pass 2 (PP2)	0.018	0.27
Bullfrog (BF)	0.087	1.5
Bullfrog/Tram (BF/TR)	0.066	0.38
Tram 1 (TR1)	0.28	1.2
Tram 2 (TR2)	0.029	0.23
Tram 3 (TR3)	0.045	2.2
Tram 4 (TR4)	0.011	0.32
Lithic Ridge 1 (LR1)	0.041	2.9
Lithic Ridge 2 (LR2)	0.027	0.83
Bow Ridge	0.018	0.50

Figure 2-8. Darcy flux vector plots for vertical cross section flow model

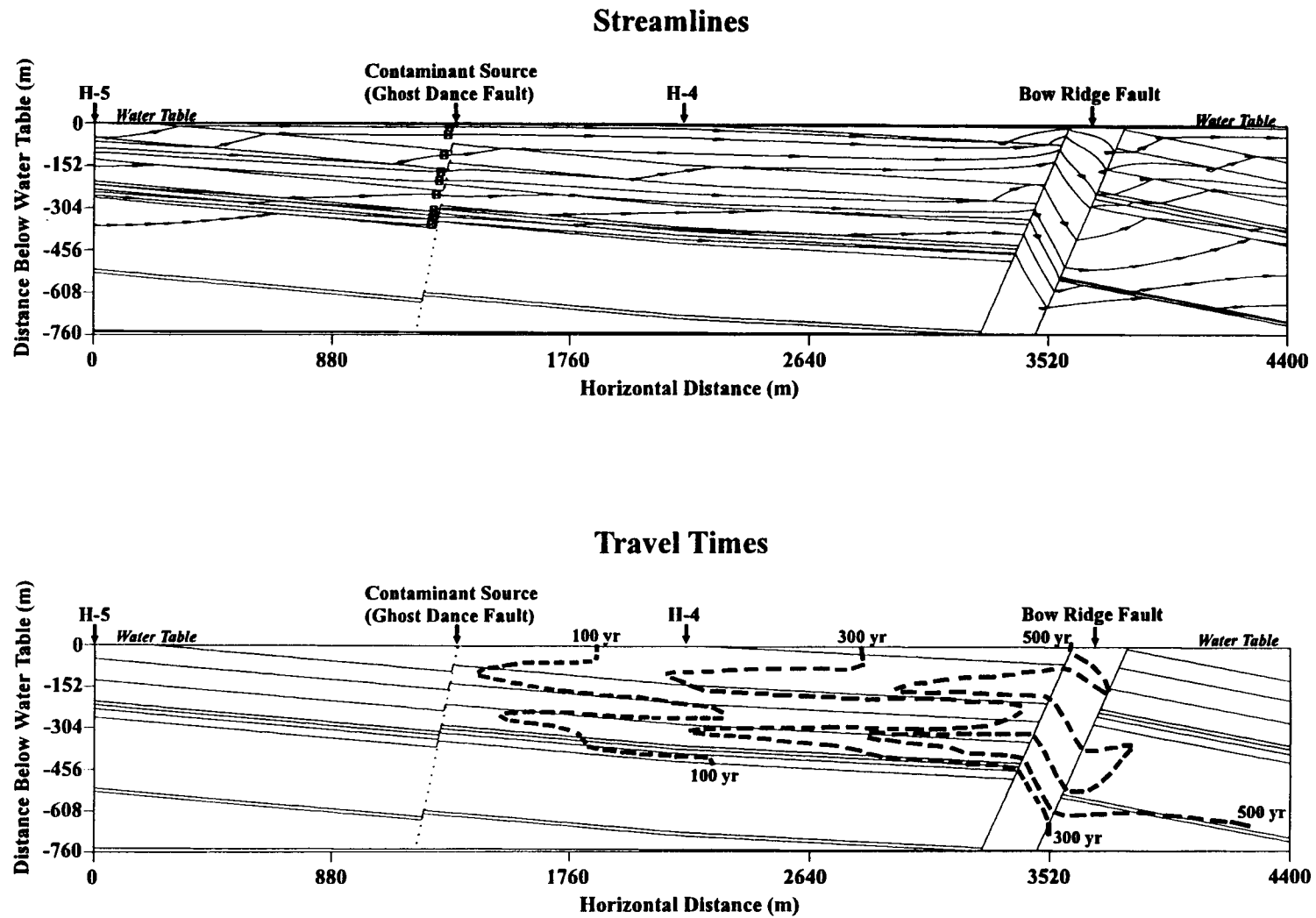


Figure 2-9. Pathlines and particle travel times for vertical cross-section flow model

10/29

The previously inferred trends of contaminant movement are clearly illustrated in the contour plot of the <sup>99</sup>Tc plume shown in figure 2-10; the isopleths in this case are expressed in terms of dilution factors. Plume representations for two snapshots in time (i.e., times of 200 and 1,000 yr after release) are shown in the figure. The computer simulation results suggest there is relatively little local mixing and dilution (i.e., dilution factor of about 2) near the contaminant source. The plot for 1,000 yr clearly illustrates two important points: (i) the contaminant plumes remain relatively undiluted near the water table surface and (ii) structural features such as the Bow Ridge fault can indeed produce significant vertical spreading of the contaminant plume.

### 3 ASSUMPTIONS AND LIMITATIONS

#### 3.1 CONCEPTUAL MODELS

The reliability of the dilution factor estimates presented herein depend, to a very large degree, on the appropriateness of groundwater flow conceptualizations implemented in the numerical models. Much direct and indirect evidence (e.g., hydrostratigraphy, head gradients, and temperature profiles) suggests a relatively complex 3D flow system in the tuff aquifer. For example, the general lateral groundwater flow in the tuff aquifer, which appears to primarily occur through interconnected shear fracture zones (Geldon, 1993), can be interrupted by upward flow (or upwelling) in the vicinity of faults [e.g., upward flow along splays of the Solitario Canyon fault (Wilson, et al., 1994)]. In developing conceptual models for this scoping analysis, a number of simplifying assumptions were made regarding:

- dimensionality of the conceptual model
- hydraulic conductivity and mass dispersivity tensors
- heterogeneity and spatial variability of hydraulic properties.
- hydraulic boundary conditions

As discussed previously, 2D conceptual models were adopted to simplify the modeling task. The reduced dimensionality of the conceptual models used in this analysis is significant in that mixing processes in the third dimension are neglected which results in underestimating the degree of dilution. This limitation may be particularly significant in the lateral flow model where the plume was assumed to be confined to a 10 m mixing depth because of the 2D assumption. In the actuality, vertical mixing of the plume would occur over the long flow path length (i.e., more than 30 km), dispersing the plume over much greater depths and enhancing dilution. In the case of the vertical flow model, the 2D assumption is probably less significant because of the short path length of the flow domain.

In the 2D models, the tensorial nature of hydraulic conductivity and mass dispersivity was simplified by assuming the principal directions were aligned with the coordinate axes. While this assumption is convenient (i.e., the cross terms of the tensors become zero) and commonly employed, it reduces the ability of the models to capture important directional characteristics of the flow field. These simplifications, however, are typically conservative with respect to dilution because certain aspects of hydrodynamic dispersion are neglected. Further conservatism was introduced by choosing mass dispersivities ( $\alpha_L$  and  $\alpha_T$ ) that are expected to be on the low side relative to values reported in the literature (Gelhar et al., 1985).

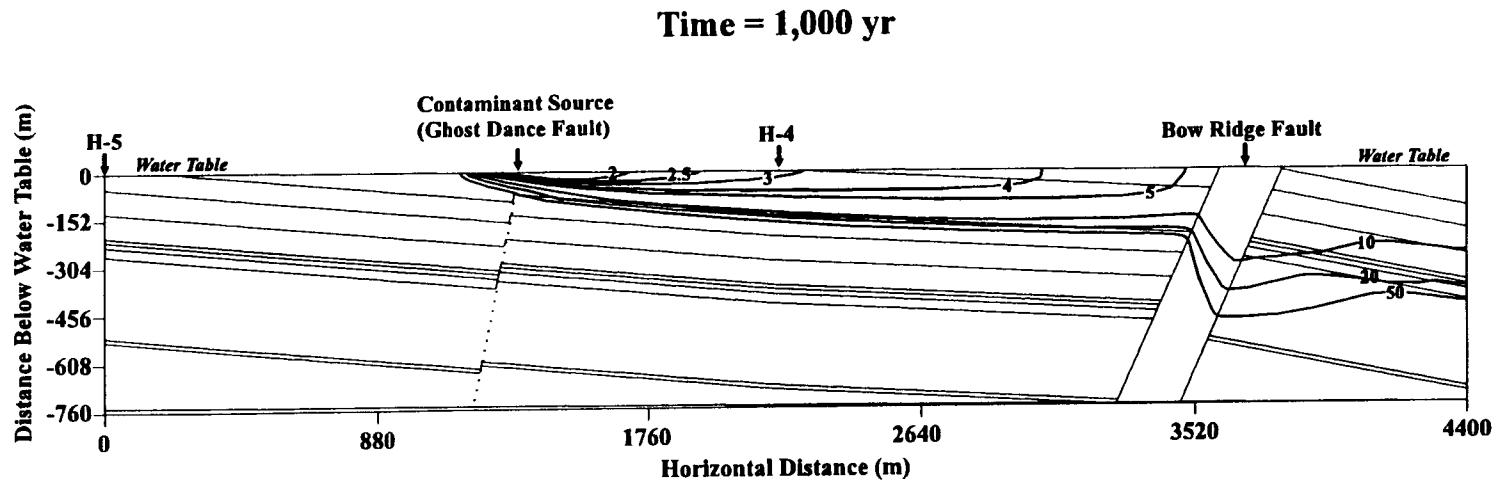
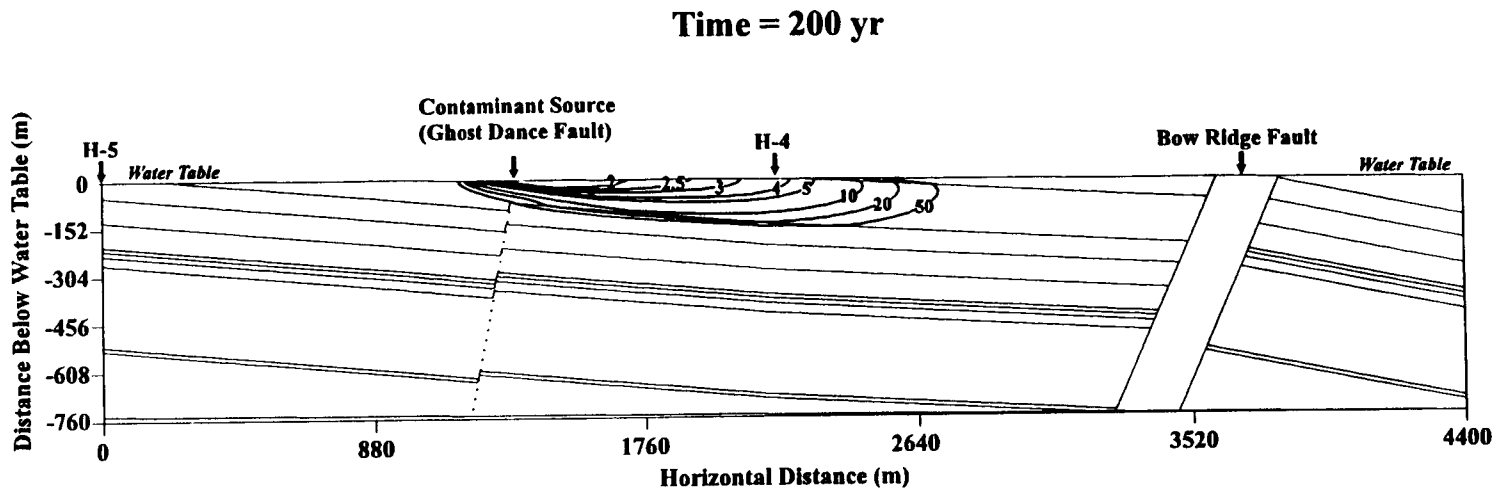


Figure 2-10. Radionuclide plume distributions for vertical cross section model with contour levels in terms of dilution factors

6/1/10

Available site data indicate that the actual groundwater system exhibits much heterogeneity and spatial variability. Hydraulic conductivities of relatively large spatial regions and individual hydrostratigraphic units were assumed uniform in both the lateral and vertical flow models. This assumption of homogeneous regions and strata is consistent with simplifications made in recent DOE 3D groundwater flow analyses (Wilson et al., 1994; Arnold and Barr, 1996), however, it is significant to analysis of mixing processes (as well as to flow paths and particle travel times). Effects of heterogeneity were indirectly taken into account through the use of mass dispersivities, but nevertheless the homogeneity assumption probably leads to an underestimation of dilution.

The current sparsity of data required making certain assumptions regarding of the hydraulic boundary conditions for both the lateral and vertical flow models. The hydraulic heads assigned to the inflow and outflow boundaries of the lateral flow model are consistent with field data, however, the side boundaries were assumed to be no-flow boundaries. The no-flow assumption may be tenuous in the vicinity of the Amargosa Farms area where water well pumping probably affects flow patterns as may interbasin transfers. In the case of the vertical flow model, the uniform head profile assigned to the inflow boundary (at USW H-5) is probably not accurate because this is a region of likely upward flow; the true head profile at this boundary probably exhibits distinct vertical gradients. How significantly these types of assumptions affect the dilution effects is uncertain at this time.

One of the fundamental assumptions made is that the hydraulics of the groundwater system can be modeled as an equivalent porous medium. This assumption is probably quite defensible for the alluvial aquifer (lower portion of the lateral flow model) but potentially weak for the tuff aquifer (upper portion of lateral flow model). Dual porosity or dual permeability models (National Research Council, 1996) may provide more realistic representations of hydraulic and transport behavior of fracture zones in the tuff formations. For at least one borehole at YM, the dual porosity approach has been shown to yield a better interpretation of pump test data (Moench, 1984).

### 3.2 HYDRAULIC AND TRANSPORT PROPERTIES

At present, there is considerable data for the hydraulic and transport properties of the unsaturated zone at YM. Much of this unsaturated zone data is documented in Flint and Flint (1990), Wittwer et al. (1995), Rautman et al. (1995), Schenker et al. (1995), and Flint et al. (1996) which has been used in various subsystem performance assessments (Arnold and Barr, 1996; Arnold et al., 1996; Ho et al., 1996) and total-system performance assessments (Wilson et al. 1994; TRW Environmental Safety Systems Inc., 1995). In contrast, the amount of field data available for the saturated zone is limited, particularly for parameters necessary for dilution calculations. These data are not only insufficient in amount but also in spatial coverage.

In the conduct of this scoping analysis, past and recent USGS reports on field testing conducted in the tuff aquifer were reviewed to compile necessary data. Other borehole data for the alluvial aquifer were also examined. Particular attention was placed on identifying data for estimation of

- hydraulic heads and gradients
- hydraulic conductivities

- effective porosities
- mass dispersivities.

Most hydraulic head data (from which head gradients may be calculated) available for the YM site is in terms of composite heads (i.e., vertically averaged heads). As such, these data do not provide a means of estimating vertical head gradients. Hydraulic conductivity profiles such as those measured in USW H-4 (Whitfield et al., 1985) provide a good indication of the range of values for the horizontal component  $K_{xx}$  of the conductivity tensor. At present, there are no data to estimate the vertical component  $K_{zz}$ . There are no field data for effective porosities or mass dispersivities, but the USGS is currently evaluating tracer tests in the C-well complex (Geldon, 1995) expected to yield such data. At the subregional scale, there are again composite head data but no known data for hydraulic conductivity, effective porosity, or mass dispersivities.

### 3.3 RADIONUCLIDE SOURCE TERM

The calculation of the radionuclide release from a repository generally requires the application of a detailed source term and release model (Sagar et al., 1992) that takes into account such factors as the engineered barrier design, thermohydrologic conditions, near-field chemistry, and drift scale flow conditions. For the purposes of this scoping analysis, a simple approach for calculating the  $^{99}\text{Tc}$  release to groundwater was adopted. In this approach, the release was computed assuming a fractional release rate of  $10^{-5}$  /yr, a mixing depth of 10 m, and 50 percent of the waste packages failed. This simple calculation of the source term assumed no dilution of  $^{99}\text{Tc}$  in the unsaturated zone and that the radionuclide instantaneously reached the saturated zone. For the lateral flow case, three separate source locations on the periphery of the repository were assumed for the purpose of creating distinct plumes. For the vertical cross section model, source locations adjacent to the Ghost Dance fault were assumed; these source zones spanned a distance of about 120 m on each side of the fault. No uncertainties or parameter variations in the radionuclide source term were examined. These assumptions are significant when interpreting the calculational results.

## 4 SUMMARY OF ANALYSIS RESULTS

### 4.1 GROUNDWATER FLOW PATHS AND PARTICLE TRAVEL TIMES

Computer visualizations of flow paths for the two conceptualizations of 2D groundwater flow provided a preliminary understanding of flow patterns. For example, the simulations of lateral flow in regional groundwater flow systems indicated that, depending on the hydraulic characteristics of faults (such as Bow Ridge fault), streamlines depict either flow across and along the fault zone or alternatively, flow completely around it. Such observations are consistent with the hydraulic head field generally orienting itself to move water along the most conductive components of the hydrogeologic system. Similarly, the simulations for the vertical flow conceptual model (based on the cross section through USW H-5 and USW H-4) suggested that the streamlines in the aquifer beneath the proposed repository generally follow hydrogeologic units with higher hydraulic conductivity. This trend was only altered by the presence of fault zones that caused refraction and spreading of streamlines.

Particle travel time ( $t_p$ ) calculations for both the vertical flow and lateral flow models highlighted the sensitivity to location of the particle release point and hydraulic conductivities and effective porosity values. For example, release points on the northeastern boundary of the repository foot print appear to follow the longer flow paths whereas those on the southern boundary trace out more direct paths with shorter particle travel times. Order of magnitude estimates of particle travel times were calculated for the assumed upper bound values (see 2.1.1) for effective porosities:

- lateral flow model (from edge of repository to Amargosa Farms):  $t_p \sim 10^4$  yr
- vertical flow model (from Ghost Dance fault to Bow Ridge fault):  $t_p \sim 500$  yr

It is important to note that the calculation of particle travel times is very sensitive to effective porosity  $\phi$  values. For instance, if the lower bound values of  $\phi$  (see 2.1.1) are assumed, the lateral flow model produces particle travel times of about 3,000 to 5,000 yr for a path length of about 30 km (to Amargosa Farms area); for equivalent  $\phi$  assumptions, the vertical flow model yields particle travel times of about 25 yr for a path length of about 3 km.

The relatively short particle travel times in the vertical flow model are consistent with conditions of fracture flow as opposed to matrix flow. The expectation of fracture flow is supported by field data (Geldon, 1993) that indicate the primary groundwater flow in the tuff aquifer occurs in fracture zones (e.g., shear fractures). It is noteworthy to mention that while some field data were used in these calculations, the deterministic analyses presented have not considered parameter uncertainties (e.g., spatial variability of hydraulic properties), flow in discrete fractures, or possible implications of matrix diffusion effects.

## 4.2 GROUNDWATER FLUXES

The ratio of moisture flux through the unsaturated zone ( $q_{UZ}$ ) to the saturated zone groundwater flux ( $q_{SZ}$ ) is a rough indicator of the bulk mixing and dilution that can potentially occur in the aquifer immediately beneath the proposed repository foot print. As shown in TRW Environmental Safety Systems Inc. (1995), a bulk mass balance can be used to derive an approximate expression for the dilution factor (DF)

$$DF = \frac{q_{sz}}{q_{UZ}} g_f \tag{1}$$

where  $g_f$  is a geometric factor computed by dividing the cross sectional flow area in the aquifer by the effective flow area of the repository. Assuming a mixing depth of 10 m, this factor is  $g_f = 0.1$ . In the Nuclear Regulatory Commission (NRC) Iterative Performance Assessment (IPA) Phase 2 study (Nuclear Regulatory Commission, 1995), the maximum unsaturated zone flux values assumed for the current and pluvial climates were  $5 \times 10^{-3}$  and  $10^{-2}$  m/yr, respectively. The flow simulations using the MAGNUM-2D code indicate groundwater fluxes (below the proposed repository) ranging from about 0.5 m/yr to approximately 2.0 m/yr. Using the above equation, a rough estimate of the range of dilution factors yields  $5 \leq DF \leq 20$ . The lower bound value is consistent with the more detailed transport calculations described in the following section.

### 4.3 DILUTION RESULTING FROM NATURAL MIXING

The overall finding of this preliminary scoping analysis was that passive groundwater mixing at the YM site is not likely to produce very large dilution factors such as those reported in TSPA-1995 (TRW Environmental Safety Systems Inc., 1995). In the immediate vicinity of the repository, dilution can be limited because the directional characteristics of the flow, magnitudes of the Darcy fluxes, or tendency for contaminant plumes to remain on or close to the water table surface. As the radionuclide plumes travel away from the proposed repository, they may tend to have a greater chance of spreading and becoming diluted both laterally and vertically as a result of movement through or around large scale structural features such as faults. Depending on their large scale hydraulic properties, faults in the tuff aquifer could play a major role in determining the rate and direction of plume spread. At substantial distances, radionuclide plumes traveling through the alluvium are expected to be further mixed with pristine waters but the dilution factors at locations such as the Amargosa Farms are unlikely to increase by many orders of magnitude, as suggested by DOE (TRW Environmental Safety Systems, Inc., 1995).

Transport simulations of hypothetical releases of <sup>99</sup>Tc (a highly mobile radionuclide with long half-life) from discrete locations in the proposed repository specifically suggest the following ranges of dilution factors:

- immediate vicinity of the repository:  $2 \leq DF \leq 5$
- great distance from the proposed repository (e.g., Amargosa Farms):  $5 \leq DF \leq 50$

It is important to acknowledge that these estimates may be relatively conservative, particularly for locations at large distances. Clearly, accurate estimates of groundwater dilution factors will not be attainable until field data for site specific transport parameters (e.g., mass dispersivities and effective porosities) are available. However, results of this scoping analysis, together with available geochemical data (Benson and McKinley, 1985; Claassen, 1985), are sufficient to argue that the actual dilution factors are not expected to be larger by many orders of magnitude. This expectation may be revised if mixing resulting from water well pumping is found to be a significant dilution process. A quantitative study of wellbore mixing and dilution will be performed in the near-term.

## 5 REFERENCES

Arnold, B.W., and G.E. Barr. 1996. Numerical modeling for saturated-zone groundwater travel time analysis at Yucca Mountain. *Proceedings of the Seventh Annual High-Level Radioactive Waste Management Conference*. La Grange, IL: American Nuclear Society: 187-189.

Arnold, B.W., S.J. Altman, T.H. Robey, R.W. Barnard, and T.J. Brown. 1996. *Unsaturated-Zone Fast-Path Flow Calculations for Yucca Mountain Groundwater Travel Time Analyses (GWTT-94)*. SAND95-0857. Albuquerque, NM: Sandia National Laboratory.

Benson, H.C., and P.W. McKinley. 1985. *Sources and Mechanisms of Recharge for Ground Water in the East-Central Amargosa Desert, Nevada—A Geochemical Interpretation*. U.S. Geological Survey Professional Paper 712-F. Washington, DC: U.S. Geological Survey.

26/29

- Carrera, J., and S.P. Neuman. 1986a. Estimation of aquifer parameters under transient and steady-state conditions, 1. Maximum likelihood method incorporating prior information. *Water Resources Research* 22(2): 199-210.
- Carrera, J., and S.P. Neuman. 1986b. Estimation of aquifer parameters under transient and steady-state conditions, 2. Uniqueness, stability, and solution algorithms. *Water Resources Research* 22(2): 211-227.
- Carrera, J., and S.P. Neuman. 1986c. Estimation of aquifer parameters under transient and steady-state conditions, 3. Application to synthetic and field data. *Water Resources Research* 22(2): 228-242.
- Claassen, H.C. 1985. *Sources and Mechanisms of Recharge for Ground Water in the West-Central Amargosa Desert, Nevada—A Geochemical Interpretation*. U.S. Geological Survey Professional Paper 712-F. Washington, DC: U.S. Geological Survey.
- Czarnecki, J.B. 1985. *Simulated Effects of Increased Recharge on the Ground-Water Flow System of Yucca Mountain and Vicinity, Nevada—California*. U.S. Geological Survey Water-Resources Investigations Report WRI-84-4344. Denver, CO: U.S. Geological Survey.
- Czarnecki, J.B., and R.K. Waddell. 1984. *Finite-Element Simulation of Groundwater Flow in the Vicinity of Yucca Mountain, Nevada—California*. Water Resources Investigations Report WRI-84-4349. Denver, CO: U.S. Geological Survey.
- Domenico, P.A., and F.W. Schwartz. 1990. *Physical and Chemical Hydrogeology*. New York, NY: John Wiley and Sons.
- England, R.L., K.J. Ekblad, and R.G. Baca. 1985. *MAGNUM-2D Computer Code: Users Guide*. RHO-BW-CR-143. Richland, WA: Rockwell International.
- Erickson, J.R., and R.K. Waddell. 1985. *Identification and Characterization of Hydrologic Properties of Fractured Tuff Using Hydraulic and Tracer Tests—Test Well USW H-4, Yucca Mountain, Nevada*. U.S. Geological Survey. Water Resources Investigations Report WRI-85-4066. Denver, CO: U.S. Geological Survey.
- Ervin, E.M., R.R. Luckey, and D.J. Burkhard. 1993. Summary of revised potentiometric-surface map for Yucca Mountain and vicinity, Nevada. *Proceedings of the Fourth Annual High-Level Radioactive Waste Management*. La Grange, IL: American Nuclear Society: 1,554-1,558.
- Fetter, C.W. 1993. *Contaminant Hydrogeology*. New York, NY: MacMillan Publishing Company.
- Flint, L.E. and A.L. Flint. 1990. *Preliminary Permeability and Water-Retention Data for Nonwelded and Bedded Tuff Samples*. U.S. Geological Survey. Open-File Report. USGS/OFR-90-569. Denver, CO: U.S. Geological Survey.

Flint, L.E., A.L. Flint, C.A. Rautman, and J.D. Istok. 1996. *Physical and Hydrologic Properties of Rock Outcrop Samples at Yucca Mountain, Nevada*. Open-File Report USGS/OFR-95-280. Denver, CO: U.S. Geological Survey.

Freeze, R.A., and J.A. Cherry. 1979. *Groundwater*. Englewood Cliffs, NJ: Prentice Hall, Inc.

Geldon, A.L. 1993. *Preliminary Hydrogeologic Assessment of Boreholes UE-25c #1, UE-25c #2, and UE-25c #3, Yucca Mountain, Nye County, Nevada*. Denver, CO: U.S. Geological Survey.

Geldon, A.L. 1995. *Results and Interpretation of Preliminary Aquifer Tests in Boreholes UE-25c #1, UE-25c #2, and UE-25c #3, Yucca Mountain, Nevada*. U.S. Geological Survey Water-Resources Investigations Report WRI94-4177. Washington, DC: U.S. Geological Survey.

Gelhar, L.W. 1993. *Stochastic Subsurface Hydrology*. Englewood Cliffs, NJ: Prentice Hall, Inc.

Gelhar, L.W., A. Mantoglou, C. Welty, and K.R. Rehfeldt. 1985. *A Review of Field-Scale Physical Solute Transport Processes in Saturated and Unsaturated Porous Media*. EPRI EA-4190. Palo Alto, CA: Electric Power Research Institute.

Gillson, R.G., III, P.S. Adams, J.S. Hand, and S.J. Lawrence. 1995. A computer hydrogeologic model of the Nevada Test Site and surrounding region. *Geological Society of America 1995 Annual Meeting. Abstracts*. Boulder, CO: Geological Society of America: A-187.

Ho, C.K., S.J. Altman, and B.W. Arnold. 1996. *Alternative Conceptual Models and Codes for Unsaturated Flow in Fractured Tuff: Preliminary Assessments for GWTT-95*. SAND95-1546, Albuquerque, NM: Sandia National Laboratory.

Kline, N.W., and R.G. Baca 1985. *CHAI NT Computer Code: Users Guide*. RHO-BW-CR-144. Richland, WA: Rockwell International.

LaPlante, P.A., M.S. Jarzemba, R.B. Neel, and C.A. McKenney. 1996. *An Initial Approach for Defining Potential Site-Specific Reference Biospheres and Critical Groups for Exposure Scenarios*. San Antonio, TX: Center for Nuclear Waste Regulatory Analyses.

Moench, A.F. 1984. Double porosity models for a fissured groundwater reservoir with fracture skin. *Water Resource Research*. 20(7): 831-846.

National Research Council. 1995. *Technical Bases for Yucca Mountain Standards*. Washington, DC: National Academy Press.

National Research Council. 1996. *Rock Fractures and Fluid Flow*. Washington, DC: National Academy Press.

Neuman, S.P. 1975. Analysis of pumping test data from anisotropic unconfined aquifers considering delayed gravity response. *Water Resources Research* 11(2): 329-342.

- Nuclear Regulatory Commission. 1995. *Phase 2 Demonstration of the NRC's Capability to Conduct a Performance Assessment for a High-Level Waste Repository*. NUREG-1464. Washington, DC: Nuclear Regulatory Commission.
- Rautman, C.A., L.E. Flint, A.L. Flint, and J.D. Istok. 1995. *Physical and Hydrologic Properties of Rock Outcrop Samples from a Nonwelded Tuff Transition, Yucca Mountain, Nevada*. Water-Resources Investigation: Report 95-4061. Denver, CO: U.S. Geological Survey.
- Roberson, K.E., E.H. Price, and S.J. Lawrence. 1995. Simplification of the geologic framework of the Nevada Test Site and surrounding region for a hydrogeologic computer model. *Geological Society of America 1995 Annual Meeting. Abstracts*. Boulder, CO: Geological Society of America: A-187.
- Robison, J.H. 1984. *Ground-Water Level Data and Preliminary Potentiometric Surface Map of Yucca Mountain and Vicinity, Nye County, Nevada*. Water Resources Investigations Report WRI84-4197, Denver, CO: U.S. Geological Survey.
- Robison, J.H., and R.W. Craig. 1991. *Geohydrology of Rocks Penetrated by Test Well USW H-S, Yucca Mountain, Nye County, Nevada*. Water Resources Investigations Report WRI88-4168. Denver, CO: U.S. Geological Survey.
- Sagar, B., R.B. Codell, J.C. Walton, and R.J. Janetzke. 1992. *SOTEC: A Source Term Code for High-Level Waste Geologic Repositories Users Manual, Version 1.0*. CNWRA 92-009. San Antonio, TX: Center for Nuclear Waste Regulatory Analyses.
- Schenker, A.R., D.C. Guerin, T.H. Robey, C.A. Rautman, and R.W. Barnard. 1995. *Stochastic Hydrogeologic Properties Development for Total-System Performance Assessments*. SAND94-0244. Albuquerque, NM: Sandia National Laboratory.
- Scott, R.B., and J. Bonk. 1984. *Preliminary Geologic Map of Yucca Mountain with Geologic Sections, Nye County, Nevada*. U.S. Geological Survey Open-File Report OFR84-494. Denver, CO: U.S. Geological Survey.
- Snow, D.T. 1969. Anisotropic permeability of fractured media. *Water Resources Research* 5(6): 1,273-1,289.
- TRW Environmental Safety Systems, Inc. 1995. *Total System Performance Assessment—1995: An Evaluation of the Potential Yucca Mountain Repository*. B00000000-01717-2200-00136, Rev. 01. Las Vegas, NV: TRW Environmental Safety Systems Inc.
- Walker, G.E., and T.E. Eakin. 1963. *Geology and Ground-Water of Amargosa Desert, Nevada—California, Ground-Water Resources Reconnaissance Series Report 14*. Carson City, NV: State of Nevada Department of Conservation and Natural Resources.
- Whitfield, M.S., E.P. Eshom, W. Thordarson, and D.H. Schaefer. 1985. *Geohydrology of Rocks Penetrated by Test Well USW H-4, Yucca Mountain, Nye County, Nevada*. Water-Resources Investigations Report WRI-85-4030. Denver, CO: U.S. Geological Survey.

- Wilson, M.L., J.H. Gauthier, R.W. Barnard, G.E. Barr, H.A. Dockery, E. Dunn, R.R. Eaton, D.C. Guerin, N. Lu, M.J. Martinez, R. Nilson, C.A. Rautman, T.H. Robey, B. Ross, E.E. Ryder, A.R. Schenker, S.A. Shannon, L. H. Skinner, W.G. Haley, J.D. Gansemer, L.C. Lewis, A.D. Lamont, I.R. Triay, A. Meijer, and D.E. Morris. 1994. *Total-System Performance Assessment for Yucca Mountain—SNL Second Iteration (TSPA-93)*. SAND93-2675, Vol. 1 & 2. Sandia National Laboratory, Albuquerque, NM.
- Wittmeyer, G.W. 1990. *Robust Estimation of Parameters in Nonlinear Subsurface Flow Models Using Adjoint State Methods*. Ph.D. Dissertation. Tucson, AZ: University of Arizona.
- Wittmeyer, G.W., and S.P. Neuman. 1992. Monte-Carlo experiments with robust estimation of aquifer model parameters. *Advances in Water Resources* 14: 252-272.
- Wittwer, C., G. Chen, G.S. Bodvarsson, M. Chornack, A. Flint, L. Flint, E. Klicklis, and R. Spengler. 1995. *Preliminary Development of the LBL/USGS Three-Dimensional Site Scale Model of Yucca Mountain, Nevada*. LBL-37356, UC-814. Berkeley, CA: Lawrence Berkeley Laboratory.